CDC01-REG1559

Stability and reachability analysis of a hybrid model of luminescence in the marine bacterium *Vibrio fischeri*

Calin Belta[1], Jonathan Schug, Thao Dang
Vijay Kumar, George J. Pappas, Harvey Rubin,
University of Pennsylvania, Philadelphia, PA, USA
and
Paul Dunlap
University of Michigan, Ann Arbor, MI, USA

Abstract

This paper addresses the mathematical modeling and analysis of the quorum sensing system found in unicellular bacteria that exhibit bioluminescence. The luminescence is governed by the expression of genes in the cell, which in turn is controlled by the density of cells in a population. The paper illustrates the application of standard tools in control theory and some recent tools in hybrid systems to the quorum sensing system, and demonstrates that bioluminescence can be modeled and understood as the output of a switched, dynamic system.

1 Introduction

We have recently seen the sequencing of the human genome and we know now that the human body is effectively controlled and regulated by 30,000 genes. However, we are yet to develop the ability to model, analyze, and predict the effect of the products of specific genes and genetic networks on cell and tissue function. The main goals of our research are to create the enabling technologies and develop the scientific techniques that are necessary to understand and predict the integrated functions of cellular regulatory networks, and to model and abstract principles of organization, design, control, and coordination in these networks.

A good illustration of a multicellular network is the cell-density-dependent gene expression seen in prokaryotes. In this process, a single cell is able to sense when a *quorum* of bacteria, a minimum population unit is achieved. Under these conditions, certain behavior is efficiently performed by the quorum, such as bioluminescence, the best known model for understanding the mechanism of cell-density-dependent gene expression.

This phenomenon of quorum-sensing is recognized now in over 25 species of Gram-negative bacteria, including several pathogens of animals and plants, where it regulates production of extracellular enzymes, transfer of plasmids, synthesis of antibiotics, and formation of biofilms [8, 21].

Our goal in this paper is to develop and analyze a model for the genetic regulatory apparatus in a marine bacterium, *Vibrio fischeri*, which colonizes the light organ of the bobtailed squid, *Euprymna scolopes*. During the day, the squid remains buried in the sand of shallow reef flats. As the sun sets, the nocturnal animal emerges from its safe hiding place and searches for food. In the moonlit night, the squid would appear as a dark silhouette and be easily detected by predatory fish from below. It is thought that the squid camouflages itself by projecting light

[1] GRASP Laboratory, 3401 Walnut St., Philadelphia, PA 19104-6228, Tel:(215) 898-5814

downward from its light organ. This is made possible by the colonization of the light organ by the luminescent bacteria, *Vibrio fischeri*.

The luminescence is connected to a complex quorum-sensing mechanism, involving multiple genes for signal generation and signal response, as well as various cellular inputs that influence the timing and level of activity of the quorum-sensing mechanism [9, 20, 22]. Quorum sensing coordinates the production of several proteins of diverse functions in *V. fischeri* [5]. Certain of these proteins, possibly including those for luminescence, apparently are involved in the bacterium's ability to colonize its symbiotic host animal [5, 24].

Our approach to understanding the *V. fischeri* quorum-sensing system couples standard, well-known tools in control theory (controllability and stability of nonlinear systems) [15] with some recent tools that have been developed for *hybrid systems theory.* A hybrid system is a dynamic system that consists of discrete and continuous components with complex interactions (cf. [3, 13, 23, 17]). The hybrid models in the paper can also be thought as *switched systems* [18]. We will be interested mainly in studying the stability of possible equilibrium points and in questions of reachability of our switched system model. Reachability analysis can be used to establish biological properties of cellular networks. For example, one can ask if a single *V. fischeri* bacterium in the right environment can multiply and eventually reach a steady state of luminescence. In our work, this translates to the reachability of an equilibrium of a discrete mode of the hybrid system.

In this paper, we develop and analyze models for luminescence in two forms of *V. fischeri.* We consider an isolate from nature (*wild type*) with the native quorum-sensing intact and a mutant strain of this species [9] that is defective in one of the key regulatory elements of the system. We first develop a continuous model for the biochemical reactions in the wild type, using numerical simulation to study the quorum sensing phenomenon in Section 3. We next develop a hybrid abstraction of the same phenomenon in Section 4. This hybrid model lends itself to the computation of equilibrium points and the analytical study of stability of the equilibrium points. The reachability analysis of a luminescent equilibrium in a mutant is developed in Section 5. Finally, we formulate our conclusions and suggest future work.

2 Regulation of bioluminescence in *Vibrio fischeri*

Vibrio fischeri is a marine bacterium which can be found both as free-living organism and as a symbiont of some marine fish and squid. As a free-living organism, *V. fisheri* exists at low densities and appears to be non-luminescent. As a symbiont, the bacteria live at high densities and it is, usually, luminescent. In a liquid culture, the bacterium's level of luminescence is low until the culture reaches mid to late exponential phase. Later, in stationary phase, the level of bioluminescence decreases. This luminescence is controlled by the transcriptional activation of the *lux* genes in the bacterium.

The *lux* regulon [20] is organized in two transcriptional units, O_L and O_R. See Figure 1. The leftward operon, O_L, contains the *luxR* gene encoding the protein [2] LuxR, a transcriptional regulator of the system. The rightward operon O_R contains seven genes *luxICDABEG.* The transcription of the *luxI* gene results in the production of protein LuxI. This protein is required for endogenous production of *autoinducer*, *Ai*, a small membrane-permeant signal molecule (acyl-homoserine lactone). The genes *luxA* and *luxB* code for the luciferase subunits, and *luxC*, *lux D*, and *lux E* code for polypeptides of the fatty-acid reductase, which generates aldehyde substrate for luciferase. The *luxG* gene is thought to encode a flavin reductase. Along with LuxR and LuxI, cAMP receptor protein (CRP)

[2] We use italics (*e.g.*, *luxR*) to indicate the genes and plain font to denote the protein expressed by the gene (*e.g.*, LuxR)

plays an important role in controlling luminescence.

The network of biochemical reactions in the cell is as follows. The autoinducer Ai binds to protein LuxR to form a complex Co which binds to the *lux box* shown in Figure 1. The *lux box* is in the middle of a regulatory region between the two transcriptional units (operons). This region also contains a binding site for CRP. According to Dunlap [19], the transcription from the *luxR* promoter is activated by the binding of CRP to its binding site, and the transcription of the *luxICDABEG* by the binding of Co to the *lux box*. However, growth in the levels of Co and cAMP/CRP inhibit *luxR* and *luxICDABEG* transcription, respectively. These feedback loops are shown through dotted arrows with '+' and '-' signs in Figure 1.

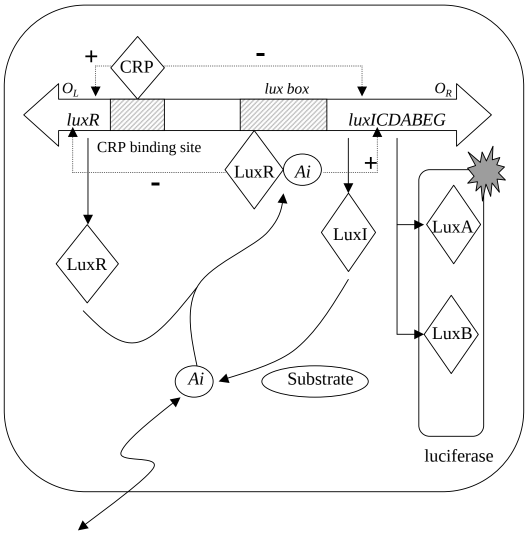

Figure 1: A portion of DNA showing the *luxR* (transcribed from the leftward operon O_L) and *luxICDABEG* (transcribed from the rightward operon O_R) genes and the binding sites for complex Co and CRP

In this paper, we develop a mathematical model for quorum sensing for bioluminescence in *V. fischeri* that is derived from the literature in microbiology [9, 20, 22, 19, 8, 21]. It is important to recognize that our approach to modeling is phenomenological and not exact. The models for biochemical molecular reactions follows standard approaches used in chemical reaction thermodynamics, despite the complexity associated with bindings of macromolecules to geometrically complex binding sites and the low molecular concentrations that may be encountered during the evolution of the dynamic system. We also note that the growth models that are used in this paper are only a first attempt to mathematically model the experimental observations made by microbiologists in our group and elsewhere.

3 Continuous mathematical model

Our mathematical model for the luminescence phenomenon in a single *V. fischeri* cell incorporates the concentrations of the relevant mRNAs, proteins and other chemical compounds. Our model of population growth assumes that all bacteria are similar. The equations are based on the competition model as described in [9].

We use the following generic formula for any molecular species (mRNA, protein, protein complex, small molecule)

[25]:

$$\frac{d[x]}{dt} = synthesis - decay \pm transformation \pm transport$$

The *synthesis* term represents transcription for mRNA and translation for proteins. The *decay* category represents a first order degradation process. Many molecules undergo *transformations* such as cleavage or ligand-binding reactions. Finally, many molecules participate in *transport* processes, like diffusion through a membrane.

A typical gene has a single promoter, but multiple regulatory sites, both activating and inhibiting, distributed through a regulatory region. We model the regulation using functions traditionally found in biological literature [12]:

$$\Phi(X, \kappa_{Xm}, \nu_{Xm}) = \frac{X^{\nu_{Xm}}}{\kappa_{Xm}^{\nu_{Xm}} + X^{\nu_{Xm}}}, \tag{1}$$

$$\Psi(X, \kappa_{Xm}, \nu_{Xm}) = 1 - \Phi(X, \kappa_{Xm}, \nu_{Xm}). \tag{2}$$

where X is the concentration of some species with regulatory effect on the transcription of mRNA m. ν_{Xm} is called the cooperativity coefficient and κ_{Xm} is the concentration of X at which transcription of m is "half-maximally" activated. The graph of function Φ, the so called *sigmoid*, is given for illustration in Figure 2.

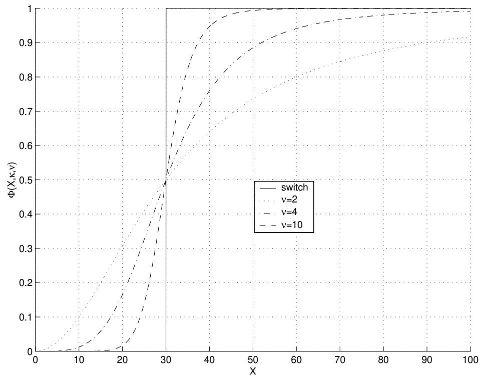

Figure 2: The function $\phi(X, \kappa, \nu)$ for $\kappa = 30$ along with a piecewise continuous abstraction

To model the luminescence phenomenon in *V. fischeri*, we restrict our attention to a nine dimensional state space, each component (with the exception of the population x_0) denoting the appropriate nano-molar concentration. This model is derived from the observations documented in [9]. The full model is described by:

$$\begin{aligned}
\dot{x}_0 &= k_G x_0 \\
\dot{x}_1 &= T_c(\Psi(x_8, \kappa_{Co-icdabeg}, \nu_{Co-icdabeg})\Phi(c_{\mathrm{CRP}}, \kappa_{\mathrm{CRPr}}, \nu_{\mathrm{CRPr}}) + b) - \frac{x_1}{H_{\mathrm{RNA}}} - k_G x_1 \\
\dot{x}_2 &= T_c(\Phi(x_8, \kappa_{\mathrm{Co-icdabeg}}, \nu_{\mathrm{Co-icdabeg}})\Psi(c_{\mathrm{CRP}}, \kappa_{\mathrm{CRPr}}, \nu_{\mathrm{CRPr}}) + b) - \frac{x_2}{H_{\mathrm{RNA}}} - k_G x_2 \\
\dot{x}_3 &= T_l x_1 - x_3/H_{\mathrm{sp}} - r_{\mathrm{AIR}} x_7 x_3 + r_{\mathrm{Co}} x_8 - k_G x_3 \\
\dot{x}_4 &= T_l x_2 - x_4/H_{\mathrm{sp}} - k_G x_4 \\
\dot{x}_5 &= T_l x_2 - x_5/H_{\mathrm{sp}} - k_G x_5 \\
\dot{x}_6 &= T_l x_2 - x_6/H_{\mathrm{up}} - k_G x_6 \\
\dot{x}_7 &= x_0(r_{\mathrm{AII}} x_4 - r_{\mathrm{AIR}} x_7 x_3 + r_{\mathrm{Co}} x_8) - x_7/H_{\mathrm{AI}} \\
\dot{x}_8 &= r_{\mathrm{AIR}} x_7 x_3 - x_8/H_{\mathrm{sp}} - r_{\mathrm{Co}} x_8 - k_G x_8
\end{aligned} \tag{3}$$

where

$$k_G = k_g(1 - x_0/x_{0\max})$$

and

$$\begin{aligned}
x_0 &= \text{scaled population (population} \times v_b/V),\\
x_1 &= \text{mRNA transcribed from } O_L,\\
x_2 &= \text{mRNA transcribed from } O_R,\\
x_3 &= \text{protein LuxR},\\
x_4 &= \text{protein LuxI},\\
x_5 &= \text{protein LuxA/B},\\
x_6 &= \text{protein LuxC/D/E},\\
x_7 &= \text{autoinducer } Ai,\\
x_8 &= \text{complex } Co.
\end{aligned}$$

The parameters in model (3) are given in Table 1. We determined the parameters in several ways. The maximum transcription and translation rates were extracted from [16] as was the half-life of RNA. The half-lives of proteins were set relatively high as they are stable [9]. The basal transcription rate was set to a low value to reflect the normally off state of transcription. The volume of the bacterium was estimated from its physical dimensions. The growth rate and solution volume determining k_G and x_0 were set to the approximate growth seen in experiments described in [9]. The cooperativity coefficient $\nu_{\mathrm{Co-icdabeg}}$ was set to two since the complex binds as a dimer. ν_{CRPr} was arbitrarily set to one, since we assume constant levels of CRP (CRP is not a state variable). The κ_* values were estimated based on expected concentrations and adjusted to yield good behavior. The rate constants r_{AII}, r_{AIR}, and r_{Co} were estimated based on expected concentrations and adjusted to yield good behavior.

The time-varying population x_0 can be viewed as a forcing function in an otherwise autonomous system. In constructing the model (3), we made the following six assumptions:

1. The population x_0 doubles in an hour under ideal conditions (verified through experimental observations [9]);
2. During growth, dilution (loss of molecules through division) applies to every molecule in the bacterium (all mRNAs and proteins);
3. The concentration of CRP is constant, thus letting $\Phi(c_{\mathrm{CRP}}, \kappa_{\mathrm{CRPr}}, \nu_{\mathrm{CRPr}})$ and $\Psi(c_{\mathrm{CRP}}, \kappa_{\mathrm{CRPr}}, \nu_{\mathrm{CRPr}})$ be constant in (3);
4. Ai diffuses rapidly through the cell membrane, so that the internal and external concentrations can be assumed to be in equilibrium at all times [9];
5. The concentration of substrate necessary for endogenous production of Ai is constant; and
6. The luminescence is due to the luciferase in the cell, which is essentially the dimer LuxA/B, whose concentration is given by x_5.

Figure 3 shows log-linear plots of numerical simulations of the continuous system for different constant concentrations of CRP. The population (bottom - right row) grows from 10^5/ml to 10^9/ml over about 15 hours then remains constant for an additional 20 hours (stable phase). Our model does not incorporate the internal changes that may occur during the stable phase if the proper physiological conditions are not maintained, but we include

Parameter	Description	Estimated Value	Units
T_c	maximum transcription rate	0.25	nM/s
T_l	maximum translation rate	0.25	1/s
H_{RNA}	RNA half life	60	s
H_{sp}	stable protein half-life	3600	s
H_{up}	unstable protein half-life	600	s
H_{AI}	*Ai* half-life	36000	s
r_{AII}	rate const. at which LuxI makes *Ai*	5e-2	1/s
r_{AIR}	rate const. *Ai* binding to LuxR	1e-6	1/nMs
r_{Co}	rate const. of *Co* dissociation	1e-2	1/s
ν_{CRPr}	cooperativity coef. for CRP	1	
κ_{CRPr}	half maximum conc. for CRP	10	nM
$\nu_{\mathrm{Co-icdabeg}}$	cooperativity coef. for *Co*	2	
$\kappa_{\mathrm{Co-icdabeg}}$	half maximum conc. for *Co*	20	nM
b	basal transcription rate	1e-5	nM/s
v_b	volume of a bacterium	1.5e-15	ℓ
V	volume of solution	1.0e-3	ℓ
k_g	growth rate	1.925e-4	1/s
$x_{0\max}$	maximum population	$10^9 \times v_b/V$	

Table 1: Model parameters - notation, description and units.

it to show the settling of the other state variables to equilibrium values. The plots of the other state variables show a more complex pattern. Common to all CRP concentrations, is a very short initial adjustment period where protein, complex, and Ai concentrations reach a nearly constant state at low population density which lasts for roughly eight hours. LuxR is abundant, ready to sense increases in Ai. On the other hand, Co, $LuxI$, and Ai are low. During this time the total luminescence is low and grows in proportion to the population. As the population grows, the total production of Ai begins to rise above the background. Rising Ai triggers the formation of LuxR:Ai complex Co. At moderate concentrations of CRP, increasing Co activates the positive feedback loop of O_R, LuxI, and Ai. The concentrations of these components increase rapidly as does the total luminescence. At higher levels of CRP the response is delayed since the extra CRP represses the induction of O_R. At low CRP concentration, the initial value of LuxR is lower and the increasing Ai is not able to form enough Co to activate the O_R feedback loop.

4 Hybrid modeling and analysis

The curve describing the regulation of transcription in Figure 2 is merely a convenient way of modeling the turning off of gene expression at low concentrations and the turning on of the gene at high concentrations. There is little experimental data confirming the exact shape of the sigmoid curve in the figure and we lack experimental data needed to estimate parameters like κ and ν (as in (1)). In the absence of such data, it is simpler to pursue piece-wise constant approximations to the function that map the degree of activation/inhibition of transcription

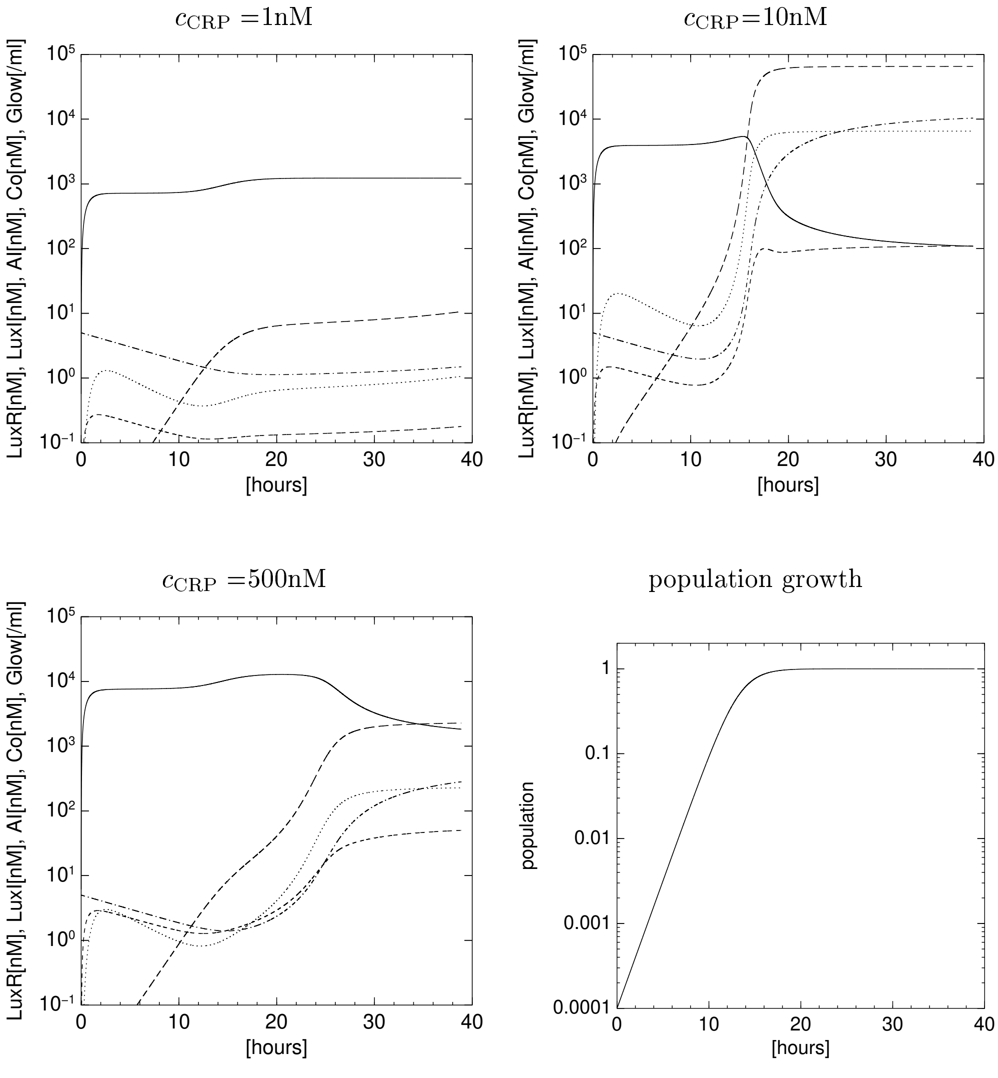

Figure 3: Time evolution of concentrations (in nM) during population growth for the continuous model: proteins LuxR (solid), LuxI (dotted), Ai (dot-dashed), Co (dashed), and total luminescence (long dashes).

of a gene to a intervals of concentration of activator/inhibitor. Figure 2 shows a 2-step model that effectively turns off the gene expression completely below a certain concentration of the regulator, and turns it on completely above that concentration. But one can also imagine a more sophisticated n-step approximation that is based on n experimental data points. From a system analysis point of view, dealing with such piecewise constant functions describing transcription is definitely advantageous, because it allows us to abstract a nonlinear system as a switched, lower dimensional, system that may be easier to analyze because of the absence of the sigmoid nonlinearity.

To fix some notation, consider the graphical illustration of a hybrid system in Figure 4. This hybrid system

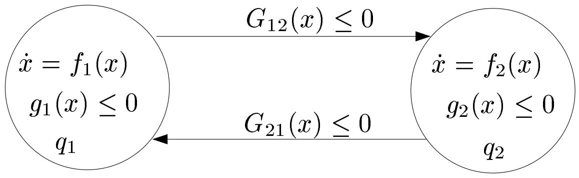

Figure 4: A simple hybrid system.

consists of two *discrete modes* q_1 and q_2, and the continuous variable x which evolves under the differential equation $\dot{x} = f_1(x)$ in discrete mode q_1, and $\dot{x} = f_2(x)$ in mode q_2. The *invariant* sets associated with the locations q_1 and q_2 are $g_1(x) \leq 0$ and $g_2(x) \leq 0$, respectively. The hybrid system continuously evolves in discrete mode q_1 according to the differential equation $\dot{x} = f_1(x)$, as long as x remains inside the invariant set $g_1(x) \leq 0$. If during the continuous flow, it happens that x belongs in the *guard* set $G_{12}(x) \leq 0$ then the transition from q_1 to q_2 is enabled. A state jumps from q_1 to q_2 and the system evolves according to the differential equation in mode q_2 as long as the invariant $g_2(x) \leq 0$ is satisfied.

The safety criticality of many embedded systems has resulted in significant research on computing reachable sets for hybrid systems. `HyTech` [14] can be used for verification of linear hybrid automata. `CheckMate` [6] and `d/dt` [7] are capable of handling more complex systems. In particular, `CheckMate` can be used for computing reachable sets for nonlinear systems of low dimension. The package `d/dt` can handle linear differential inclusions [4, 7] and lends itself to the analysis of our switched linear system.

The essential idea behind `d/dt` is to over-approximate reachable sets at each time step in the continuous phase on a step-by-step basis, as in numerical simulation. In the next section, we use `d/dt` to compute reachable sets of a hybrid model of a mutant of *V. fischeri*.

The results of a switched model obtained from (3) by replacing the sigmoids with piecewise constant functions with three steps are shown in Figure 5 for a constant CRP concentration of 10nM. The plots closely resemble the continuous simulations. The final equilibrium values are also in good agreement between the two models.

4.1 Development of a simplified hybrid model

To derive the simplified hybrid model, in addition to (1.-6.) from Section 3, we make the following assumptions:

7. We disregard the growth of the population x_0 and, consequently, the dilution. This situation corresponds to a completely grown or to a growth-controlled population.

8. mRNA has the fastest dynamics of all the molecules in bacteria (*i.e.*, H_{RNA} is small compared to other time scales). Consequently, the mRNA dynamics are assumed instantaneous.

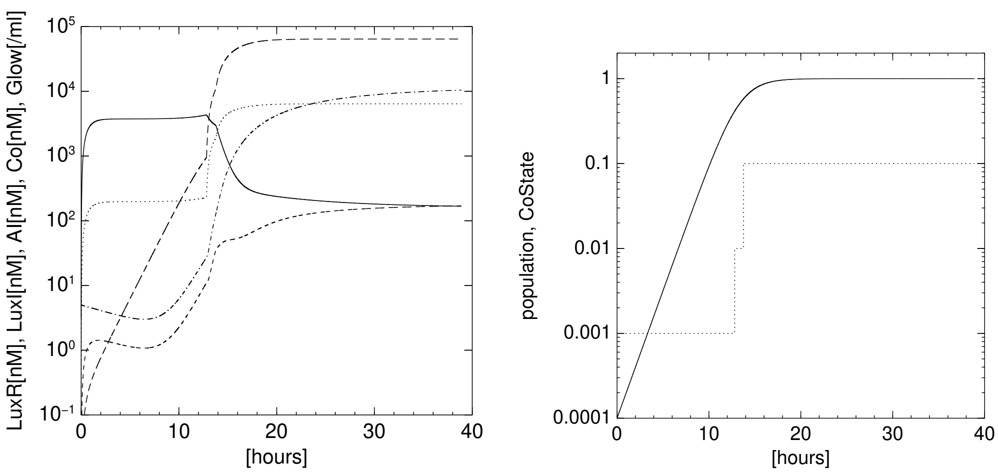

Figure 5: Time evolution of concentrations (in nM) during population growth for the switched model: proteins LuxR (solid), LuxI (dotted), Ai (dot-dashed), Co (dashed), and total luminescence (long dashes). The right figure shows the population (solid) and the switch history (dotted).

9. The gene transcription regulations are modeled as piecewise continuous functions, as shown in Figure 2.

With the above assumptions, the equations for mRNA become linear, independent of the other equations in the model. Moreover, the mRNA concentrations can be assumed to be switching among constant levels, the switching being determined by the concentrations of their corresponding activators/inhibitors. This gives a partition of the state space with specific dynamics in each region, which we will call *modes*. In each mode, the equations of the proteins which are not involved in chemical reactions are linear and lead to stable values uniquely determined by the mode. To determine the equilibria or study stability and reachability of certain states, we only need to look at the remaining nonlinear part of each mode (with product type nonlinearity only) and, if applicable, at the linear equations coupled with the nonlinear part - we will call this reduced set of equations the *non-trivial* part of the system - and at the behavior of the overall switched system.

The above ideas are illustrated for our model of luminescence in *V. fischeri*. We assume m levels of activation of the $luxICDABEG$ gene at c_0, c_1, ..., c_{m-1} with $c_0 = 0$ and $c_{m-1} = 1$. The level of activation of the $luxICDABEG$ gene is c_i when $x^i_{8sw} < x_8 < x^{i+1}_{18sw}$ where $x^0_{12sw} = 0$ and $x^m_{12sw} = \infty$. Similarly, for the $luxR$ gene, we assume n steps at d_0, d_1, ..., d_{n-1}, $d_0 = 0$, $d_{n-1} = 1$, and the activation is at level d_j when $c^j_{CRPsw} < c_{CRP} < c^{j+1}_{CRPsw}$. A generic mode labeled (ij) ($i = 1, \ldots, m-1$, $j = 1, \ldots, n-1$) has constant mRNA concentrations given by:

$$x^{ij}_1 = H_{RNA}T_c[(1-c_i)d_j + b], \;\; x^{ij}_2 = H_{RNA}T_c[c_i(1-d_j) + b]$$

The corresponding non-trivial dynamics are described by

$$\dot{x} = Ax + g(x) + b_{ij}, \;\; x = [x_3 \; x_4 \; x_7 \; x_8]^T \tag{4}$$

where

$$A = \begin{bmatrix} -\frac{1}{H_{sp}} & 0 & 0 & r_{Co} \\ 0 & -\frac{1}{H_{sp}} & 0 & 0 \\ 0 & x_0 r_{AII} & -\frac{1}{H_{AI}} & x_0 r_{Co} \\ 0 & 0 & 0 & -\frac{1}{H_{sp}} - r_{Co} \end{bmatrix}, \;\; g(x) = r_{AIR} x_7 x_3 p$$

$$p = \begin{bmatrix} -1 \\ 0 \\ -x_0 \\ 1 \end{bmatrix}, \quad b_{ij} = \begin{bmatrix} H_{RNA}T_cT_l[(1-c_i)d_j + b] \\ H_{RNA}T_cT_l[c_i(1-d_j) + b] \\ 0 \\ 0 \end{bmatrix}$$

and invariant sets given by

$$x_{8sw}^i < x_8 < x_{8sw}^{i+1} \bigwedge c_{CRPsw}^j < c_{CRP} < c_{CRPsw}^{j+1} \tag{5}$$

4.2 Stability analysis

The Jacobian of (4) at a feasible equilibrium x_e^{ij} (*i.e.*, all components are positive and the invariant (5) is satisfied) is given by:

$$J_{ij} = \begin{bmatrix} -\frac{1}{H_{sp}} - r_{AIR}x_{e7}^{ij} & 0 & -r_{AIR}x_{e3}^{ij} & r_{Co} \\ 0 & -\frac{1}{H_{sp}} & 0 & 0 \\ -x_0 r_{AIR}x_{e7}^{ij} & x_0 r_{AII} & -\frac{1}{H_{AI}} - x_0 r_{AIR}x_{e3}^{ij} & x_0 r_{Co} \\ r_{AIR}x_{e7}^{ij} & 0 & r_{AIR}x_{e3}^{ij} & -\frac{1}{H_{sp}} - r_{Co} \end{bmatrix}$$

J_{ij} has two eigenvalues at $-1/H_{sp}$ and the other two the roots of the polynomial

$$1 + H_{sp}r_{Co} + H_{sp}r_{AIR}x_{e7}^{ij} + x_0 H_{AI}r_{AIR}x_{e3}^{ij}$$

$$+(H_{AI} + H_{sp} + H_{AI}H_{sp}r_{Co} + H_{AI}H_{sp}r_{AIR}x_{e7}^{ij} + x_0 H_{AI}H_{sp}r_{AIR}x_{e3}^{ij})\lambda + H_{AI}H_{sp}\lambda^2$$

Since the coefficients of the above second order polynomial are strictly positive for all positive values of the constants, we conclude that, if a feasible equilibrium x_e^{ij} for mode (ij) exists, then it is locally asymptotically stable, for all feasible values of the parameters.

An estimate of the region of attraction can be easily constructed around the (possible) equilibrium of each mode due to the special form of the nonlinearity. By abuse of notation, let the translated state $x - x_e^{ij}$ be denoted by x again. The system describing the dynamics of mode (ij) around its equilibrium translated at the origin is of the form

$$\dot{x} = J_{ij}x + g(x) \tag{6}$$

where J_{ij} is Hurwitz. We use the vanishing perturbation technique [15] to construct an ellipsoidal region of attraction around the origin of (6), and, eventually, translate the ellipsoid back around x_e^{ij} in the original space. Let P_{ij} be the unique symmetric, positive definite solution of the Lyapunov equation $P_{ij}J_{ij} + J_{ij}^T P_{ij} = -I$. Let $V(x) = x^T P_{ij} x$ be the corresponding Lyapunov function for the linear part of (6) and a possible candidate for the nonlinear system. The derivative of $V(x)$ along the trajectories of (6) is given by:

$$\dot{V}(x) = -\|x\|^2 + 2x^T P_{ij} g(x) = -\|x\|^2 + 2r_{AIR}x_7 x_3 x^T P_{ij} p$$

If x is in the region between two hyperplanes in $\mathbb{R}^4$ containing the origin of the form $|x^T P_{ij} p| < \kappa$, then it is easy to see that $\kappa < 1/r_{AIR}$ is a sufficient condition for $\dot{V}(x) < 0$. To find an estimate for κ, we solved the constrained optimization problem

$$\max_{x,\, x^T P_{ij} x = c} |x^T P_{ij} p| = \sqrt{c}\sqrt{p^T P_{ij} p}$$

The conclusion is that the maximum ellipsoid of attraction is of the form

$$V(x) = x^T P_{ij} x \leq \frac{1}{r_{AIR}^2 p^T P_{ij} p} \tag{7}$$

If the ellipsoid described by (7) is completely included in the invariant of mode (ij), then we can conclude that it is indeed an attractive set for the switched system (4). Otherwise, it needs to be shrunk until the inclusion condition is satisfied.

A more interesting question than stability for both biologists and control engineers would be what makes the system switch among modes. For example, given a (desired, luminescent) stable equilibrium, with the above method we can construct a region of attraction within the corresponding mode, but can the ellipsoid be reached from other (non-luminescent) modes? This is a reachability problem, which we cannot solve using existing tools. However, we can solve such reachability problems for a mutant of *V. fischeri* where luminescence is described by linear switched dynamics.

5 Reachability analysis of a mutant of *V. fischeri*

In this section we model a mutant of *V. fischeri* like one described in [19] that disrupts the operon structure, and, therefore, the regulatory system described above. In the mutant, the *luxR* gene is deleted from its normal location and a copy is placed in a plasmid (a separate piece of DNA) and incorporated back into *V. fischeri.* The plasmid copy of *luxR* is under control of a different promoter that yields a constant, high rate of transcription unaffected by any of the molecules described above. We assume a constant concentration of protein LuxR at x_3 = 10000nM. The model becomes linear with non-trivial dynamics for mode (ij) in the form $\dot{x} = Ax + b_{ij}$, where $x = [x_4\ x_7\ x_8]^T$ and

$$A = \begin{bmatrix} -\frac{1}{H_{sp}} & 0 & 0 \\ x_0 r_{AII} & -\frac{1}{H_{AI}} - x_0 R r_{AIR} & x_0 r_{Co} \\ 0 & R r_{AIR} & -\frac{1}{H_{sp}} - r_{Co} \end{bmatrix}, \quad b_{ij} = \begin{bmatrix} H_{RNA} T_l T_c [c_i(1-d_j) + b] \\ 0 \\ 0 \end{bmatrix}$$

The unique equilibrium of mode (ij) is given by:

$$x_{e4}^{ij} = (b + c_i - c_i d_j) H_{RNA} H_{sp} T_c T_l$$

$$x_{e7}^{ij} = \frac{(b + c_i - c_i d_j) x_0 H_{AI} H_{RNA} H_{sp} r_{AII} (1 + H_{sp} r_{Co}) T_c T_l}{(1 + x_0 H_{AI} R r_{AIR} + H_{sp} r_{Co}}$$

$$x_{e8}^{ij} = \frac{(b + c_i - c_i d_j) x_0 H_{AI} H_{RNA} {H_{sp}}^2 R r_{AII} r_{AIR} T_c T_l}{(1 + x_0 H_{AI} R r_{AIR} + H_{sp} r_{Co}}$$

The eigenvalues of matrix A are $-1/H_{sp}$ and the roots of the second order polynomial

$$1 + x_0 H_{AI} R r_{AIR} + H_{sp} r_{Co} + (H_{AI} + H_{sp} + x_0 H_{AI} H_{sp} R r_{AIR} + H_{AI} H_{sp} r_{CO})\lambda + H_{AI} H_{sp} \lambda^2,$$

which is easily seen to be Hurwitz, for all (positive) values of the parameters. We conclude that, if an equilibrium is feasible (*i.e.*, the invariant (5) is satisfied), then it is *locally* asymptotically stable. Note that, even if the dynamics of mode (ij) are linear, we cannot decide *global* stability because of the switching. However, reachability analysis could give us insight into global properties.

Consider the case where the CRP concentration is low (regulation kept at d_0=0). The system is composed of two modes (00) and (10), which we call non-luminescent (non-lum) and luminescent (lum), respectively. For the values of the parameters given in Table 1, the equilibria are given by:

$$x_{e4}^{\text{non-lum}} = 13.5,\ x_{e7}^{\text{non-lum}} = 36.1823,\ x_{e8}^{\text{non-lum}} = 17.8434$$

and

$$x_{e4}^{\text{lum}} = 13513.5,\ x_{e7}^{\text{lum}} = 36218.5,\ x_{e8}^{\text{lum}} = 17861.2$$

Assuming that the *luxICDABEG* gene is switched on at $x_{8sw} = 1000$, both the above equilibria are feasible. An interesting question from a biological point of view would be under what conditions the system arrives at the luminescent equilibrium, and particularly, what makes the system switch and turn on the *luxICDABEG* gene?

We illustrate our approach to answer such questions by considering a simple example. To determine the states from which the system can reach the equilibrium x_e^{lum}, consider a small neighborhood F around x_e^{lum} and determine all states that can reach F by performing backward reachability analysis. We model the system as a hybrid automaton [1] with two discrete states corresponding to the two modes (see Figure 6).

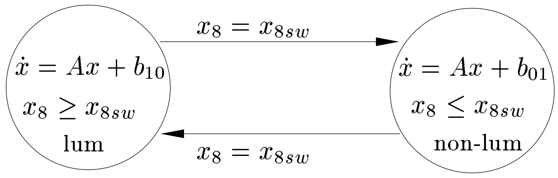

Figure 6: The hybrid automaton of the mutant system.

The reachability analysis of the mutant system is done using `d/dt` [4, 7]. Basically, `d/dt` uses polyhedra to over- or under-approximate reachable sets of hybrid automata. For our problem, an under-approximation is required since we need to make sure that all the states in the computed set go to the equilibrium x_e^{lum}. We define the neighborhood F as the box $[13500, 13525] \times [36200.0, 36230.0] \times [17860, 17868]$ and study the system's behavior within the set $[0, 30000] \times [0, 60000] \times [0, 30000]$. The tool computes first the set $\mathcal{R}_{lum}$ of states backward reachable from F by mode lum (see Figure 7 (a)). Then, to determine the states from which the system can switch to mode non-lum (backward in time), the intersection of $\mathcal{R}_{lum}$ with the switching plane $x_8 = x_{8sw}$ is computed, which gives the set $G = [0, 30000] \times [1400.2, 42926.5] \times [1000, 1000]$. Starting from the intersection, the tool computes the set $\mathcal{R}_{non-lum}$ backward reachable by mode non-lum (see Figure 7 (b)).

This example illustrates how one can predict the initial conditions under which luminescence can be achieved. While the above results of the calculation are consistent with the experimental observations, it is premature to conclude anything from this preliminary analysis. The described method merely points to a set of directions for modeling and experimental validation.

6 Conclusion

In this paper we presented tools that could be used to study stability and reachability properties of biological systems, with application to quorum sensing in the marine bacterium *Vibrio fischeri*. We showed by simulation that a growing population determines building of a small molecule called autoinducer Ai and, eventually, luminescence. We presented how a reduced, hybrid model of the regulatory network can be constructed and emphasized its usefulness. Using `d/dt`, a safety verication tool for hybrid linear systems, we derived sufficient conditions for reachability of the stable luminescent state.

Programming of stochastic, networked hybrid systems can be facilitated by a specialized high-level programming language based on modern software engineering concepts. Our first step in this direction is represented by

(a) (b)

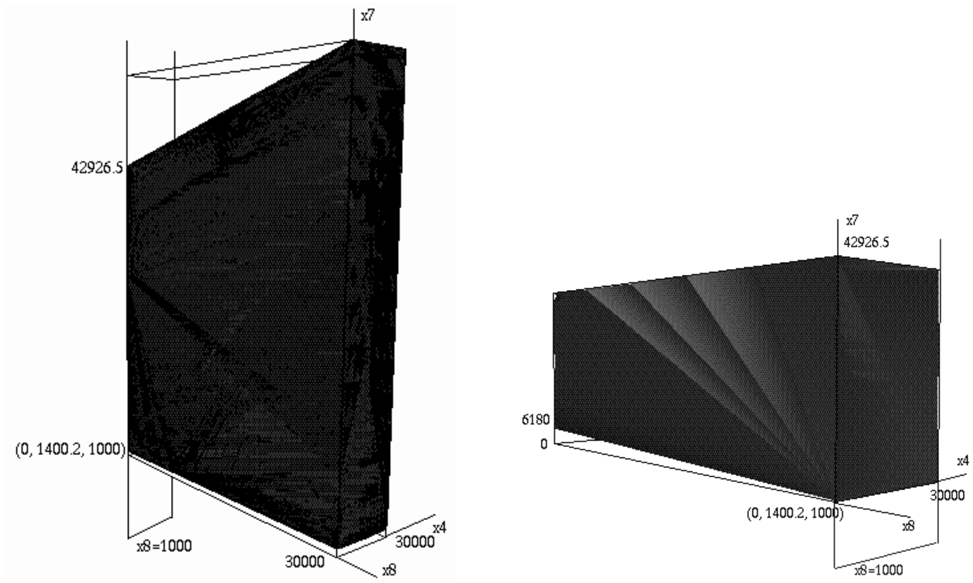

Figure 7: (a) The set $\mathcal{R}_{lum}$ of states backward reachable by mode lum (the box F is hidden inside $\mathcal{R}_{lum}$); (b) The set $\mathcal{R}_{non-lum}$ of states backward reachable by mode non-lum (the set G is the rectangle on the switching plane $x_8 = 1000$).

the language, Charon, a language designed for networked hybrid systems that supports hierarchy, modularity, specification of mixed discrete-continuous behavior, and communication primitives for networks [2]. The stochastic modeling of hybrid systems and the appropriate extensions to Charon are important future directions.

Also relevant to this research on modular simulation in which hierarchical, hybrid systems can be simulated efficiently with guarantees on accuracy [10, 11]. Hybrid system models for biology and for robotics will be characterized by thousands of differential equations with hundreds of modes and inequality constraints. Accuracy guarantees are extremely important in hybrid systems. Unlike continuous or discrete systems, small errors in detecting the violation of unilateral constraints can completely change the ensuing time history of the state. An important direction of future work is the development of a set of tools for developing hierarchical, hybrid abstractions, and for automated modular, multi-rate simulation of large-scale biological networks.

7 Acknowledgments

This paper is part of a large collaborative effort that includes Rajeev Alur, Franjo Ivancic, Insup Lee, and Max Mintz. Charon and its development is a collaboration between SDRL and GRASP laboratories at the University of Pennsylvania and is supported by funding from DARPA ITO Mars and Mobies programs.

References

[1] R. Alur, C. Courcoubetis, N. Halbwachs, T.A. Henzinger, P.-H. Ho, X. Nicollin, A. Olivero, J. Sifakis, and S. Yovine. The algorithmic analysis of hybrid systems. *Theoretical Computer Science*, 138:3–34, 1995.

[2] R. Alur, R. Grosu, Y. Hur, V. Kumar, and I. Lee. Modular specifications of hybrid systems in charon. *Proceedings of Third Intl. Workshop on Hybrid Systems: Computation and Control LNCS*, 1790:6–19, 2000.

[3] R. Alur, T.A. Henzinger, and E.D. Sontag, editors. *Hybrid Systems III: Verification and Control*. LNCS 1066. Springer-Verlag, 1996.

[4] E. Asarin, O. Bournez, T. Dang, and O. Maler. Approximate reachability analysis of piecewise-linear dynamical systems. In B. Krogh and N. Lynch, editors, *Hybrid Systems: Computation and Control*, Lecture Notes in Computer Science 1790, pages 20–31. Springer-Verlag, 2000.

[5] S. M. Callahan and P. V. Dunlap. LuxR- and acyl-homoserine-lactone-controlled non-*lux* genes define a quorum-sensing regulon in *Vibrio fischeri*. *J. Bacteriol.*, 182:2811–2822, 2000.

[6] A. Chutinam and B. Krogh. Verification of polyhedral-invariant hybrid automata using polygonal flow pipe approximations. In F. Vaandrager and J. H. van Schuppen, editors, *Hybrid Systems : Computation and Control*, volume 1569 of *Lecture Notes in Computer Science*. Springer Verlag, 1999.

[7] T. Dang. *Verification and Synthesis of Hybrid Systems*. PhD thesis, Institut National Polytechnique de Grenoble, Laboratoire Verimag, 2000.

[8] P. V. Dunlap. *N*-Acyl-L-homoserine lactone autoinducers in bacteria: unity and diversity. In J. A. Shapiro and M. Dworking, editors, *Bacteria as multicellular organisms*, pages 69–106. Oxford University Press, New York, 1997.

[9] P. V. Dunlap. Quorum regulation of luminescence in *Vibrio fischeri*. In D. Bartlett, editor, *Molecular marine microbiology*, pages 3–21. Horizon Press, Norfolk, UK, 2000.

[10] J. Esposito and V. Kumar. Efficient dynamic simulation of robotic systems with hierarchy. To be Presented International Conference on Robotics and Automation 2001.

[11] J. Esposito, V. Kumar, and G. Pappas. Accurate event detection for simulating hybrid systems. In *Hybrid Systems : Computation and Control*, Lecture Notes in Computer Science. Springer Verlag, 2001. To Appear.

[12] R. Heinrich and S. Schuster. *The regulation of cellular systems*. International Thomson Publishing, New York, 1996.

[13] T. Henzinger and S. Sastry, editors. *Hybrid Systems: Computation and Control*. LNCS 1386. Springer, 1998.

[14] T.A. Henzinger, P.-H. Ho, and H. Wong-Toi. A user guide to HYTECH. In E. Brinksma, W.R. Cleaveland, K.G. Larsen, T. Margaria, and B. Steffen, editors, *TACAS 95: Tools and Algorithms for the Construction and Analysis of Systems*, volume 1019 of *Lecture Notes in Computer Science 1019*, pages 41–71. Springer-Verlag, 1995.

[15] H. Khalil. *Nonlinear Systems*. Prentice Hall, Upper Sadle River, NJ, 2nd edition, 1996.

[16] B. Lewin. *Genes VII.* Oxford University Press, 7th edition, 1999.

[17] N. Lynch and B.H. Krogh, editors. *Hybrid Systems: Computation and Control.* LNCS 1790. Springer, 2000.

[18] S. Morse, editor. *Control Using Logic-Based Switching*, volume 222 of *Lecture Notes in Control and information sciences.* Springer-Verlag, 1997.

[19] P. V. Dunlap and A. Kuo. Cell density-dependent modulation of the *Vibrio fischeri* luminescence system in the absence of autoinducer and LuxR protein. *J Bacteriol*, 174(8):2440–8., 1992.

[20] D. M. Sitnikov, J. B. Schineller, and T. O. Baldwin. Transcriptional regulation of bioluminescence genes from *Vibrio fischeri. Molecular microbiology*, 17(5):801–812, 1995.

[21] S. Swift, P. Williams, and G. S. A. B. Steward. N-acylhomoserine lactones and quorum sensing in proteobacteria. In G. Dunny and S. C. Winans, editors, *Bacteria as multicellular organisms*, pages 291–313. American Society for Microbiology, Washington, DC, 1997.

[22] S. Ulitzur and P. V. Dunlap. Regulatory circuitry controlling luminescence autoinduction in *Vibrio fischeri. Photochem. Photobiol.*, 62:625–632, 1995.

[23] F. Vaandrager and J. van Schuppen, editors. *Hybrid Systems: Computation and Control.* LNCS 1569. Springer, 1999.

[24] K.L. Visick, J. Foster, J. Doino, M. McFall-Ngai, and E.G. Ruby. *Vibrio fischeri lux* genes play an important role in colonization and development of the host light organ. *Bacteriol*, 182(16):4578–4586, August 2000.

[25] G. von Dassow, E. Meir, E. M. Munro, and G. M. Odell. The segment polarity network is a robust development module. *Nature*, 406:188–192, 2000.